EUROFUSION WPMAT-PR(15) 14366

D Terentyev et al.

Modelling irradiation-induced softening in BCC Iron by crystal plasticity approach

Preprint of Paper to be submitted for publication in Journal of Nuclear Materials

This work has been carried out within the framework of the EUROfusion Consortium and has received funding from the Euratom research and training programme 2014-2018 under grant agreement No 633053. The views and opinions expressed herein do not necessarily reflect those of the European Commission.

Modelling irradiation-induced softening in BCC Iron by crystal plasticity approach

Xiazi Xiao[1,3], Dmitry Terentyev[2*] , Long Yu[1], Dingkun Song[1], A. Bakaev[2] and Huiling Duan[1,3*]

[1]*State Key Laboratory for Turbulence and Complex System, Department of Mechanics and Engineering Science, College of Engineering, Peking University, Beijing 100871, PR China*

[2]*Structural Material Group, Institute of Nuclear Materials Science, SCK·CEN, Mol, Belgium*

[3]*CAPT, HEDPS and IFSA Collaborative Innovation Center of MoE, Peking University, Beijing 100871, PR China*

Abstract

Crystal plasticity model (CPM) for BCC iron to account for radiation-induced strain softening is proposed. CPM is based on the plastically-driven and thermally-activated removal of dislocation loops. Atomistic simulations are applied to parameterize dislocation-defect interactions. Combining experimental microstructures, defect-hardening/absorption rules from atomistic simulations, and CPM fitted to properties of non-irradiated iron, the model achieves a good agreement with experimental data regarding radiation-induced strain softening and yield stress increase under neutron irradiation.

Keywords: Iron, dislocation, defect, temperature, plastic deformation

*Authors for correspondence. Email: dterenty@SCKCEN.BE; hlduan@pku.edu.cn

BCC Iron (Fe) is the basis for a class of structural steels for nuclear applications, hence being a primary model material to understand the strain-softening phenomenon, believed to be linked with plastic slip localization (PSL) and the formation of slip bands (called "clear channels" - CCs) [1-5]. Earlier experiments have shown that already at 0.1 dpa (displacement per atom) a well pronounced radiation-induced softening (RIS) takes place [6]. As expected, investigation of as-deformed microstructure reveals the occurrence of CCs being free of dislocation loops (DLs) [1, 6].

While rigorous atomistic and dislocation dynamics computations are needed to characterize the principle mechanisms provoking initiation and propagation of CCs [5, 7], matching this detailed knowledge to a computational engineering level requires the coarse grain approach such as CPM [8, 9]. For example, Patra and McDowell [8, 9] have proposed a constitutive CPM to consider the mechanical response of irradiated BCC metals addressing creep and localized deformation by absorption of immobile DLs on the basis of geometrical condition. Here, we make a step further and develop CPM to account for the DL-induced hardening and thermally-stress activated absorption of DLs in the course of plastic deformation, following the mechanisms extracted and activation function directly from atomistic simulations. We apply this model to Fe by computing the stress-strain response of neutron irradiated polycrystalline using the elastic-viscoplastic self-consistent (EVPSC) theory [10, 11].

Dealing with BCC lattice, we consider 24 slip systems ($\frac{1}{2}$<111>{110} and $\frac{1}{2}$<111> {112} types), and the plastic shear rate is set to follow the standard power-law kinetics [12]:

$$\dot{\gamma}^{\alpha}(T) = \dot{\gamma}_0 \left(\frac{\tau^{\alpha}}{\tau_c^{\alpha}(T)}\right)^m \mathrm{sign}(\tau^{\alpha}), \tag{1}$$

where $\dot{\gamma}_0$ and m are the reference shear rate and material rate sensitivity exponent, respectively. τ^{α} and $\tau_{\mathrm{c}}^{\alpha}$ represent the resolved and critical resolved shear stress (RSS and CRSS) in a particular slip system, respectively. $\tau_{\mathrm{c}}^{\alpha}$ consists of several operating hardening mechanisms, namely, the intrinsic lattice friction resistance τ_0, dislocation forest hardening $\tau_{\mathrm{n}}^{\alpha}$, irradiation defect hardening $\tau_{\mathrm{d}}^{\alpha}$ and grain boundary hardening τ_{HP}, i.e.

$$\tau_{\mathrm{c}}^{\alpha}(T) = \tau_0(T) + \tau_{\mathrm{n}}^{\alpha}(T) + \tau_{\mathrm{d}}^{\alpha}(T) + \tau_{\mathrm{HP}}(T). \tag{2}$$

It is well known that dislocation-mediated plastic flow in BCC metals is defined by the thermally activated motion of screw lines. Therefore, the temperature dependent lattice friction is considered as [13], $\tau_0(T) = (\mathrm{A} - \mathrm{B} \cdot T)^2$. The Hall-Petch effect [14, 15] is expressed as $\tau_{\mathrm{HP}}(T) = k_{HP}(T)D^{-\frac{1}{2}}$, where D is the grain size, and k_{HP} is a material constant. The dislocation forest hardening is considered as the Taylor-type hardening model, $\tau_{\mathrm{n}}^{\alpha}(T) = b\mu(T)\sqrt{h_{\mathrm{n}}\rho_{\mathrm{n}}^{\alpha}(T)}$, where b is the magnitude of the Burgers vector, and h_{n} is the hardening coefficient characterizing network dislocation interactions. $\mu(T)$ is the temperature dependent shear modulus, which is calculated as

$\mu(T) = \sqrt{C_{44}(T)\big(C_{11}(T) - C_{12}(T)\big)/2}$ using available experimental data for elastic constants [16].

The evolution of dislocation density on each particular slip system, $\dot{\rho}_{\mathrm{n}}^{\alpha}(T)$, is described by the balance of multiplication and recovery/storage following [17]:

$$\dot{\rho}_{\mathrm{n}}^{\alpha}(T) = \dot{\gamma}^{\alpha}(T)\left(k_1\sqrt{\rho_{\mathrm{n}}^{\alpha}(T)} - k_2^{\alpha}(\dot{\varepsilon},T)\rho_{\mathrm{n}}^{\alpha}(T)\right), \tag{3}$$

where k_1 and k_2^{α} are interlinked following Beyerlein and Tome [18] as:

$$\frac{k_2^{\alpha}(\dot{\varepsilon},T)}{k_1} = \frac{\chi b}{g^{\alpha}}\left(1 - \frac{k_B T}{D^{\alpha} b^3}\ln\left(\frac{\dot{\varepsilon}}{\dot{\varepsilon}_0}\right)\right), \tag{4}$$

here χ, g^{α}, D^{α}, $\dot{\varepsilon}_0$ are respectively, the interaction parameter, normalized activation energy, proportionality constant and reference strain rate.

The above described constitutive equations are parameterized using available experimental and theoretical data [19], and several parameters are fitted to reproduce the stress-strain response of Fe single crystals. The adopted parameterization set is provided in the supplementary material. In Fig. 1, the calculated stress-strain diagram demonstrates good agreement with experimental data [19] and with recent atomistic-based CPM from [20] for the <111> and <110> loading directions.

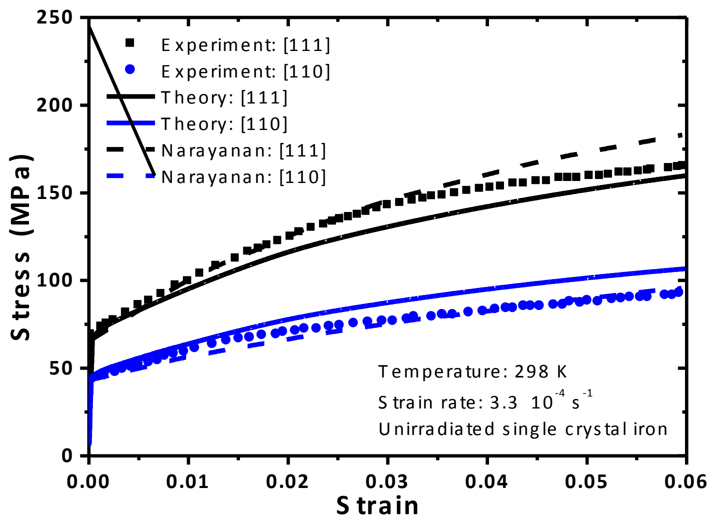

Fig. 1. The orientation dependent stress-strain curves for non-irradiated single crystal iron, compared

with experimental data [19] and atomistic-based CPM from [20].

The hardening contribution of irradiation defects (here, interstitial DLs) is accounted for via the dispersed barrier model [11] as:

$$\tau_{\mathrm{d}}^{\alpha}(T) = b\mu(T)\sqrt{h_{\mathrm{d}}\sum_{j=1}^{N_l}\mathbf{N}^{\alpha}:\mathbf{H}^{j}\,(T)}, \tag{5}$$

where h_{d} is the loop strength, and $\mathbf{N}^{\alpha}:\mathbf{H}^{j}$ gives the contact density between the DLs and dislocations. $\mathbf{N}^{\alpha}$ is defined as $\mathbf{N}^{\alpha} = \mathbf{n}^{\alpha} \otimes \mathbf{n}^{\alpha}$, with $\mathbf{n}^{\alpha}$ the normal vector of dislocation slip plane. N_l denotes the number of defect habit planes (i.e. four in the case of ½<111> DLs). $\mathbf{H}^{j}$ is the damage descriptor tensor and takes the form:

$$\mathbf{H}^{j}(T) = \rho_{\mathrm{d}}(T)\cdot 3d_l\cdot\mathbf{M}^{j}, \text{ with } \mathbf{M}^{j} = \mathbf{I_2} - \mathbf{m^j}\otimes\mathbf{m^j} \tag{6}$$

where ρ_{d}, d_l and $\mathbf{m^j}$ denote the volume density of the defect loops, its diameter and the unit normal vector, respectively. $\mathbf{I_2}$ represents the second-order unit tensor.

The core component of the CPM is the treatment of the DL – dislocation interaction resulting in the conditional absorption of loops. Following atomistic simulation data [21], ½<111> DLs are absorbed by moving dislocations in two steps: (i) the formation of a <100> junction segment (JS) and (ii) its propagation across the loop surface. Thereby, the DL can be completely absorbed into a superjog on the edge dislocation or into a helical turn on the screw dislocation. The absorption is controlled by the JS propagation, which is a stress-assisted and thermally-activated process [22]. The relation between the activation energy and effective stress ($\Delta G - \tau_{\mathrm{eff}}$) was calculated and parameterized as a function for nanometric ½<111> DLs in [21]. Note that very small DLs (clusters of several self-interstitials) do not offer any strong resistance to dislocation glide, as revealed by atomistic simulations. We shall use the $\Delta G - \tau_{\mathrm{eff}}$ function from [21] to compute the absorption frequency, ω^{α}, as:

$$\omega^{\alpha}(T) = \frac{b}{d_l}\nu_{\mathrm{D}}\exp\left(-\frac{\Delta G(\tau_{\mathrm{eff}}^{\alpha})}{k_B T}\right), \tag{7}$$

where ν_D is the Debye frequency. Assuming a homogeneous distribution of DLs, τ_{eff} can be calculated according to the force balance as:

$$\tau_{\mathrm{eff}}^{\alpha} = \frac{d_s}{d_l}(\tau^{\alpha} - \tau_0), \tag{8}$$

where $d_s = 1/\sqrt[3]{\rho_{\mathrm{d}}}$ is the spacing between DLs, d_l is the loop size; and $(\tau^{\alpha} - \tau_0)$ is the residual stress ensuring the dislocation curvature (the lattice friction τ_0 is subtracted). For a given interaction time interval τ, the cumulative distribution probability of survival (i.e. resistance to absorption) can be written as [23]:

$$P^{\alpha}(\tau < t) = 1 - \exp(-\omega^{\alpha} t). \tag{9}$$

Treating the absorption of each DL as an independent Bernoulli process within an integration time *t,* the number of accomplished absorption events obeys the binomial distribution n~B(N, p). Therefore, the DL annihilation rate equals to the survival probability:

$$\eta^{\alpha}(T) = [1 - \exp(-\omega^{\alpha}(T)\Delta t_1^{\alpha}(T))] \tag{10}$$

where Δt_1^{α} is the defect-dislocation interaction time. The evolution of the damage descriptor takes the form:

$$\dot{\mathbf{H}}^j(T) = -\sum_{\alpha=1}^{N_s} \frac{\eta^{\alpha}(T)}{\Delta t^{\alpha}(T)} \cdot \left(\mathbf{N}^{\alpha} : \mathbf{H}_{\mathrm{eff}}^j(T)\right) \cdot \mathbf{M}^j, \tag{11}$$

where $\mathbf{H}_{\mathrm{eff}}^j$ is the effective damage descriptor with the form as

$$\mathbf{H}_{\mathrm{eff}}^j(T) = \mathbf{H}^j(T) - f_s \mathbf{H}_0^j, \tag{12}$$

where f_s is the fraction of stable DLs. Finally, the time Δt_2^{α} required for the unpinned dislocation to reach the next DLs (assuming regular square array of DLs) is defined as:

$$\Delta t_2^\alpha = \frac{d_s}{v^\alpha(T)} = \frac{d_s}{\frac{\dot{\gamma}^\alpha(T)}{b\rho_n^\alpha(T)}} = \frac{b\rho_n^\alpha(T)d_s}{\dot{\gamma}^\alpha(T)}. \tag{13}$$

Hence, the total interaction time increment in Eq. (11) is $\Delta t^\alpha = \Delta t_1^\alpha + \Delta t_2^\alpha$.

Using the above formulated CPM and EVPSC method [10], we treat the experimental data of neutron irradiated Fe at 295 K up to 0.1 dpa [24]. A parameter set and its justification can be found in the supplementary material. The comparison of experimental and computed stress-strain curves is presented in Fig. 2. One can see a good agreement between the model prediction and experimental data regarding the strain-hardening curves for both non-irradiated and irradiated tests [6, 25]. Analysis of the dislocation density evolution reveals that the higher the yield stress, the faster the dislocation density saturates. The intensive dislocation multiplication, in turn, establishes a high level of shear stress in slip systems oriented closely to the maximum RSS plane, and *nominally heterogeneous* absorption of the DLs is initiated there. Thereby plastically-induced defect absorption reduces the DL density with a subsequent softening. Further increase of strain activates the DL absorption in secondary slip systems. Continuous repetition of these events is globally seen as a reduction in the strain-hardening rate.

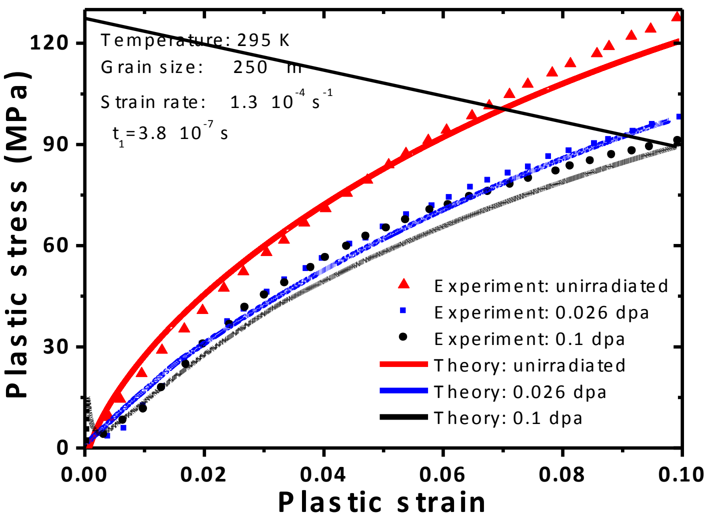

Fig. 2. Comparison of model prediction and experimental data for the plastic stress-strain response of

non-irradiated and irradiated polycrystalline iron.

To underline the impact of the plastically-induced defect absorption, the DL contribution to the macroscopic flow stress is presented in Fig. 3. Since the absorption process is both stress-induced and temperature-activated, increasing the test temperature leads to a more pronounced reduction in τ_d and its faster saturation. The saturation of loop absorption originates from the reduction of local stress acting on loops, which now is not high enough to initiate the loop absorption. Hence, Fig. 3 reveals an important conclusion, namely: increasing test temperature (or decreasing loading rate) can enhance the absorption rate provoking strain-induced softening. If the initial irradiation hardening is high, an abrupt reduction in the flow stress is likely for the low strain rate tensile tests.

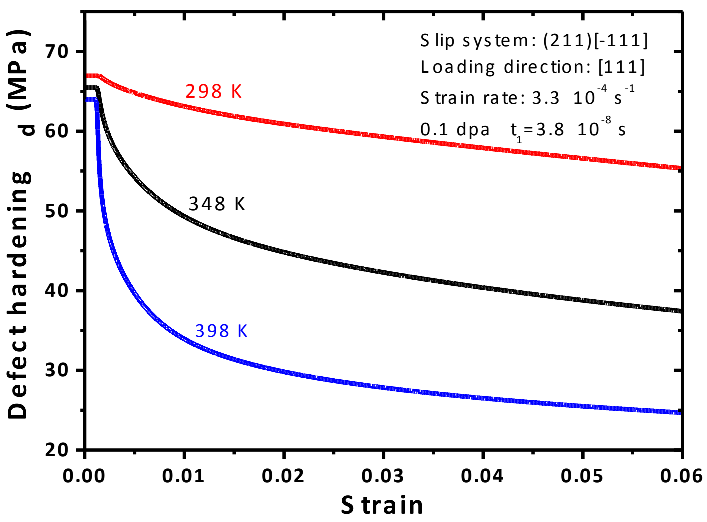

Fig. 3. The evolution of dislocation-defect interaction strength at different temperatures.

To summarize, we have proposed a multi-scale scheme to model the thermo-mechanical response of irradiated metals. Here, we focused on the stress- and temperature-activated absorption of dislocation loops in BCC metals. On the example of BCC Fe, we demonstrated how the rigorous information on atomic- and meso-scale plasticity can be incorporated via physically-based laws in the CPM frame to take into account the irradiation induced softening in e.g. polycrystalline Fe. Basing on this model, a further step is to explore the grain-scale plastic deformation due to a combined microstructure constituting of ½<111> and <100> DLs, and nano-voids, as such a defect mixture is present at high doses and temperatures relevant for commercial power plants.

Acknowledgements

This project has received funding from the European Union's Horizon 2020 research and innovation programme under grant agreement number 633053. The views and opinions expressed herein do not necessarily reflect those of the European Commission. Duan wants to acknowledge the support from the National Natural Science Foundation of China (NSFC) under Grants 11225208.

References

[1] S.J. Zinkle, B.N. Singh, J. Nucl. Mater. 351 (2006) 269.
[2] T.S. Byun, N. Hashimoto, K. Farrell, Acta Mater. 52 (2004) 3889.
[3] T.S. Byun, K. Farrell, Acta Mater. 52 (2004) 1597.
[4] Y. Brechet, G. Canova, L.P. Kubin, Acta Mater. 44 (1996) 4261.
[5] T.D. de la Rubia, H.M. Zbib, T.A. Khraishi, B.D. Wirth, M. Victoria, M.J. Caturla, Nature. 406 (2000) 871.
[6] B.N. Singh, A. Horsewell, P. Toft, J. Nucl. Mater. 271 (1999) 97.
[7] A. Arsenlis, M. Rhee, G. Hommes, R. Cook, J. Marian, Acta Mater. 60 (2012) 3748.
[8] A. Patra, D.L. McDowell, Philos. Mag. 92 (2012) 861.
[9] A. Patra, D.L. McDowell, J. Nucl. Mater. 432 (2013) 414.
[10] X.Z. Xiao, D.K. Song, J.M. Xue, H.J. Chu, H.L. Duan, J. Mech. Phys. Solids. 78 (2015) 1.
[11] D.K. Song, X.Z. Xiao, J.M. Xue, H.J. Chu, H.L. Duan, Acta Mech. Sinica. 31 (2015) 191.
[12] D. Peirce, R.J. Asaro, A. Needleman, Acta Metall. 30 (1982) 1087.
[13] M.Z. Butt, Philos. Mag. 87 (2007) 3595.
[14] E.O. Hall, Proc. Phys. Soc. Lond. Sect. B. 64 (1951) 747.
[15] N.J. Petch, J. Iron Steel. 174 (1953) 25.
[16] Y.P. Varshni, Phys. Rev. B. 2 (1970) 3952.
[17] H. Mecking, U.F. Kocks, Acta Metall. 29 (1981) 1865.
[18] I.J. Beyerlein, C.N. Tome, Int. J. Plast. 24 (2008) 867.
[19] A.S. Keh, Philos. Mag. 12 (1965) 9.
[20] S. Narayanan, D.L. McDowell, T. Zhu, J. Mech. Phys. Solids. 65 (2014) 54.
[21] D. Terentyev, G. Monnet, P. Grigorev, Scr. Mater. 69 (2013) 578.
[22] D. Terentyev, Y.N. Osetsky, D.J. Bacon, Scr. Mater. 62 (2010) 697.
[23] G. Monnet, Philos. Mag. 91 (2011) 3810.
[24] M. Hernandez-Mayoral, D. Gomez-Briceno, J. Nucl. Mater. 399 (2010) 146.
[25] M.I. Luppo, C. Bailat, R. Schaublin, M. Victoria, J. Nucl. Mater. 283 (2000) 483.